Effective Hamiltonian in manganites: Study of the orbital and spin structures

S. Ishihara* and J. Inoue
Department of Applied Physics, Nagoya University, Nagoya 464-01, Japan

S. Maekawa
Department of Applied Physics, Nagoya University, Nagoya 464-01, Japan
and Institute for Materials Research, Tohoku University, Sendai 980-77, Japan
(Received 23 May 1996; revised manuscript received 11 October 1996)

In order to study nature of the electronic structures in manganites, the effective Hamiltonian is derived by taking the degeneracy of the e_g orbitals and the strong electron correlation into account. The spin and orbital ordered phases in the insulating states are studied in the mean-field approximation applied to the effective Hamiltonian. It is shown that the A-type antiferromagnetic state is stabilized by the magnetic interaction, which strongly depends on the bond direction, originated from the orbital ordering and the electron-electron correlation. The spin and orbital excitations are also studied by utilizing the effective Hamiltonian. The spin excitations agree well with the recent results in the neutron-scattering experiments in $LaMnO_3$. Although the numerical calculation is devoted to the insulating state, the effective Hamiltonian is relevant to the metallic state as well. [S0163-1829(97)07113-0]

I. INTRODUCTION

Manganites of perovskite structure, $A_{1-x}B_xMnO_3$ (A=La, Pr, Nd, Sm), (B=Ca, Sr, Ba) and related compounds, have recently attracted much attention, because of the colossal magnetoresistance (CMR) effect and its potential application.[1–4] It is well known that the transport phenomena in the manganites are related to the spin structure which strongly depends on a magnetic field, hole-carrier concentration, kinds of A and B cations, and so on.[5,6] Further striking phenomena such as the structural phase transition induced by the magnetic field[7] and the CMR effects near the charge ordered phase[8] were recently discovered in some of the manganites.

The mother system, $LaMnO_3$, is the A-type antiferromagnetic (A-AF) insulator where spins in Mn ions are aligned antiferromagnetically in the c direction and ferromagnetically in the ab plane.[9,10] As for the lattice, the MnO_6 octahedron is cooperatively stretched out,[11,12] and it is considered that the Mn $3d_{3x^2-r^2}$ and $3d_{3y^2-r^2}$ orbitals are alternately ordered in the crystal. Upon doping of holes, the ferromagnetic metallic state appears at low temperatures and the CMR effect is observed near the ferromagnetic transition temperature. With further increasing the concentration, the ferromagnetic transition temperature decreases and the insulating state comes out again, where the spins are aligned antiferromagnetically in all directions (G-type AF).[9,10]

The transport properties in the manganites have been studied based on the double-exchange mechanism since Zener proposed it in 1951.[13–16] Here, mobile carriers in the single e_g orbital and the Hund coupling interaction between e_g and t_{2g} spins are considered. Magnetoresistance (MR) in the strong Hund coupling case were recently investigated based on this mechanism by utilizing the dynamical mean-field approximation.[17] Effects of the Jahn-Teller (JT) lattice distortion originating from the degeneracy of the two e_g orbitals on the CMR effects and the magnetism were also intensively studied.[18–22] In these theories, however, the importance of the electron-electron interaction has not been stressed, while the interaction was suggested to be one of the important key factors to describe the transport properties in manganites.[23] Actually, the intra-atomic Coulomb interaction in the e_g orbitals estimated to be 7–8 eV (Ref. 24) is much larger than the other leading energies of the parameters in the system. To the magnetism, the importance of the electron correlation in the degenerate orbitals has been pointed out by Goodenough,[10] Kanamori,[25] and Kugel and Khomskii.[26] Because the transport properties in manganites are closely related to its magnetism, as we mentioned above, it seems to be impossible to uncover the origin of the CMR effect without correct description of magnetic properties. Nevertheless, little attention has been paid to roles of the electron correlation under the orbital degeneracy and the Hund coupling on the magnetism and the CMR effects in manganites. The purpose of this work is to reconsider the electronic and transport properties in manganites by taking the orbital degeneracy and the electron correlation, as well as the Hund coupling, into account.

In this paper, we derive the effective Hamiltonian from the generalized s-d model to study the electronic structure in manganites. In addition to the degenerate two e_g orbitals, the electron-electron interaction in the e_g orbitals is considered. The Hund coupling interaction between e_g and t_{2g} spins and the antiferromagnetic interaction between t_{2g} spins are also introduced in the Hamiltonian. As the first step of the theoretical studies based on the effective Hamiltonian, we investigate the orbital and spin structures in the insulating state. The phase diagrams and the transition temperatures of the spin and orbital orderings are examined in the mean-field approximation. The excitations are also calculated in the spin-wave approximation and compared with the experimental ones. We conclude that the orbital degree of freedom and the electron correlation are essential to describe the spin structure in $LaMnO_3$.

In Sec. II, we derive the effective Hamiltonian which is relevant to the metallic as well as insulating states. Numerical results for the insulating state calculated by using the effective Hamiltonian are presented in Sec. III. Section IV is devoted to the summary. A part of this work has been briefly described in a previous paper.[27]

II. EFFECTIVE HAMILTONIAN

The effective Hamiltonian is derived from the following generalized s-d model in the three dimensional cubic crystal structure consisting of Mn ions. This model includes degenerate two e_g orbitals in each Mn ion and the intra- and interorbital on-site Coulomb interactions, and is given by

$$H = H_{e_g} + H_{t_{2g}} + H_K . \tag{2.1}$$

The first term in the right-hand side describes electrons in the e_g orbitals and is given by

$$H_{e_g} = \epsilon_d \sum_{i,\sigma,\gamma} d^\dagger_{i\gamma\sigma} d_{i\gamma\sigma} + \sum_{\langle ij\rangle,\sigma,\gamma,\gamma'} (t_{ij}^{\gamma\gamma'} d^\dagger_{i\gamma\sigma} d_{j\gamma'\sigma} + \text{H.c.}) + U \sum_{i\gamma} n_{i\gamma\uparrow} n_{i\gamma\downarrow} + U' \sum_{i} n_{ia} n_{ib} + J \sum_{i,\sigma,\sigma'} d^\dagger_{ia\sigma} d^\dagger_{ib\sigma'} d_{ia\sigma'} d_{ib\sigma}, \tag{2.2}$$

where $d^\dagger_{i\gamma\sigma}$ is the creation operator of an electron with spin σ in one of the e_g orbitals γ, ϵ_d is the level energy of the e_g orbitals. The two e_g orbitals are assumed to be degenerate. $t_{ij}^{\gamma\gamma'}$ is the matrix element of the electron transfer between γ orbital in site i and γ' orbital in the nearest-neighbor site j, and it is estimated by the second-order perturbation with respect to the electron transfer between Mn $3d$ and O $2p$ orbitals (t_{pd}). t_{pd} is parametrized as $t_{pd} = \alpha(\gamma) V_{pd\sigma}$,[28] where α is a numerical factor and $V_{pd\sigma}$ is an overlap integral independent of the orbitals. Therefore, $t_{ij}^{\gamma\gamma'}$ is denoted by $t_{ij}^{\gamma\gamma'} = \alpha(\gamma)\alpha(\gamma') t_0$ where $t_0 (\propto V_{pd\sigma}^2)$ is treated as a parameter. U and U' are the intra- and interorbital Coulomb integrals, respectively, and $J(>0)$ is the interorbital exchange integral. The Hund coupling term H_K and the antiferromagnetic interaction term $H_{t_{2g}}$ between the nearest-neighbor t_{2g} spins in Eq. (2.1) are given by

$$H_K + H_{t_{2g}} = \frac{1}{2} K \sum_{i\gamma\sigma_1\sigma_2} \mathbf{S}_i^{t_{2g}} \cdot d^\dagger_{i\gamma\sigma_1} \boldsymbol{\sigma}_{\sigma_1\sigma_2} d_{i\gamma\sigma_2} + J^{t_{2g}} \sum_{\langle ij\rangle} \mathbf{S}_i^{t_{2g}} \cdot \mathbf{S}_j^{t_{2g}}, \tag{2.3}$$

where $\mathbf{S}^{t_{2g}}$ is the spin operator for t_{2g} electrons with $S = 3/2$, and K is defined to be positive.

Among the above energy parameters in the original Hamiltonian, the electron-electron interactions have the largest energy scale. Therefore, the effective Hamiltonian in the low-energy region is derived by excluding the doubly occupied e_g states, as follows:

$$H_{\text{eff}} = \tilde{H}_{e_g} + H_K + H_{t_{2g}}. \tag{2.4}$$

$\tilde{H}_{e_g}$ describes the electrons in the e_g orbitals, and is given by

$$\tilde{H}_{e_g} = \epsilon_d \sum_{i\sigma\gamma} \tilde{d}^\dagger_{i\gamma\sigma} \tilde{d}_{i\gamma\sigma} + \sum_{\langle ij\rangle\sigma\gamma\gamma'} t_{ij}^{\gamma\gamma'} (\tilde{d}^\dagger_{i\gamma\sigma} \tilde{d}_{j\gamma'\sigma} + \text{H.c.}) + H_{2\text{-sites}} + H_{3\text{-sites}}, \tag{2.5}$$

where $\tilde{d}_{i\gamma\sigma}$ is the annihilation operator of an electron with spin σ in γ orbital without double occupancy; $\tilde{d}_{i\gamma\sigma} = d_{i\gamma\sigma}(1 - n_{i\gamma-\sigma})(1 - n_{i-\gamma\sigma})(1 - n_{i-\gamma-\sigma})$, where $n_{i\gamma\sigma}$ is the electron number operator with spin σ in γ orbital. The first and second terms are obtained from the zeroth- and first-order perturbational processes with respect to the electron transfer. The third and fourth terms are given by the second-order perturbation. In these processes, the energies of the intermediate states are classified as $U - 2K$, $U' - J$, and $U' + J - 2K$.[27,29–31] Therefore, $H_{2\text{-sites}}$ in Eq. (2.5) is further divided into the following three terms;

$$H_{2\text{-sites}} = H_U + H_{U'-J} + H_{U'+J}. \tag{2.6}$$

Among these three terms, the second term $H_{U'-J}$ is the leading term and the explicit formula is given by

$$H_{U'-J} = -\frac{2}{U'-J} \sum_{\langle ij\rangle} \left(\tfrac{3}{4} n_i n_j + \mathbf{S}_i \cdot \mathbf{S}_j\right)\left[\left(t_{ij}^{aa\ 2} + t_{ij}^{bb\ 2}\right)\left(\tfrac{1}{4} n_i n_j - T_{iz} T_{jz}\right) - t_{ij}^{aa} t_{ij}^{bb} \left(T_{i+} T_{j-} + T_{i-} T_{j+}\right) + \left(t_{ij}^{ab\ 2} + t_{ij}^{ba\ 2}\right) \times \left(\tfrac{1}{4} n_i n_j + T_{iz} T_{jz}\right) - t_{ij}^{ab} t_{ij}^{ba} \left(T_{i+} T_{j+} + T_{i-} T_{j-}\right) - \left(t_{ij}^{ab} t_{ij}^{aa} - t_{ij}^{ba} t_{ij}^{bb}\right)\left(T_{iz} T_{j+} + T_{iz} T_{j-}\right) - \left(t_{ij}^{ba} t_{ij}^{aa} - t_{ij}^{ab} t_{ij}^{bb}\right)\left(T_{i+} T_{jz} + T_{i-} T_{jz}\right)\right], \tag{2.7}$$

where n_i is the electron number operator at site i. The explicit formulas of H_U and $H_{U'+J}$ are presented in Ref. 27. $\mathbf{S}_i$ is the spin operator of the e_g electron at site i

$$\mathbf{S}_i = \frac{1}{2} \sum_{\gamma\alpha\beta} \tilde{d}^\dagger_{i\gamma\alpha} \boldsymbol{\sigma}_{\alpha\beta} \tilde{d}_{i\gamma\beta}, \tag{2.8}$$

and $\mathbf{T}_i$ is the pseudospin operator for the orbital degree of freedom defined as

$$\mathbf{T}_i = \frac{1}{2} \sum_{\alpha\gamma\gamma'} \tilde{d}^\dagger_{i\gamma\alpha} \boldsymbol{\sigma}_{\gamma\gamma'} \tilde{d}_{i\gamma'\alpha}. \tag{2.9}$$

The eigenstates of the operator $\mathbf{T}_i$ correspond to the occupied and unoccupied e_g orbitals, for example, in the $T_z = 1/2$ and

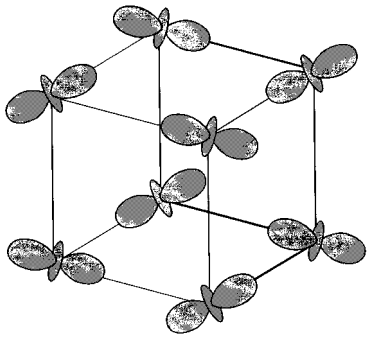

FIG. 1. The $(3x^2-r^2/3y^2-r^2)$-type orbital ordering.

$-1/2$ states, an electron occupies the $d_{x^2-y^2}$ and $d_{3z^2-r^2}$ orbitals, respectively. Each term in $H_{\text{2-sites}}$ is described by a product of spin and orbital operators, because the second-order perturbational processes simultaneously change both spin and orbital states in the i and j sites. In this sense, spin and orbital strongly couple with each other. Explicit formulas of $H_{\text{3-sites}}$ in Eq. (2.5) are not presented here, because $H_{\text{3-sites}}$ may be irrelevant as in the t-J model derived from the Hubbard Hamiltonian.

In $H_{\text{2-sites}}$, the ferromagnetic interaction between the nearest-neighboring e_g spins is originating from $H_{U'-J}$, on the other hand, the antiferromagnetic one is from $H_{U'+J}$ and H_U. As we mentioned above, $H_{U'-J}$ is a leading term in $H_{\text{2-sites}}$, because the energy prefactor $1/(U'-J)$ is largest due to the interorbital exchange interaction J and the Hund coupling interaction K. Therefore, $\tilde{H}_{e_g}$ favors the ferromagnetic spin ordering accompanied with the orbital ordering. Because the ferromagnetic interaction depends strongly on the orbital structure, the anisotropic spin structures, such as the A-type and C-type AF states, are realized by competition with the isotropic antiferromagnetic interaction caused by $H_{t_{2g}}$.

A similar model Hamiltonian with Eq. (2.6) has been proposed by Khomskii and Kugel[26] and Castellani, Natoli, and Ranninger.[32] However, effects of t_{2g} spin were not introduced in their model. Roth,[29] Cyrot and Lyon-Cean[30] and Inagaki[31] also proposed a model in the system where the orbitals are twofold degenerate. Their model coincides with ours if the matrix elements of the electron transfer are taken to be $t_{ij}^{aa}=t_{ij}^{bb}$ and $t_{ij}^{ab}=t_{ij}^{ba}=0$ in $\tilde{H}_{e_g}$. We note that the antiferromagnetic interaction between t_{2g} spins and the nonzero value of t_{ij}^{ab}, both of which are neglected in their models, are of crucial importance for stabilizing the A-AF phase in manganites, as we will show later.

III. NUMERICAL RESULTS AND DISCUSSION

In this section, we present the numerical results in the insulating phase $LaMnO_3$ calculated by utilizing the effective Hamiltonian introduced in the previous section. First, we present the phase diagrams and the transition temperatures of the spin and orbital ordered states calculated by the mean-field approximation. We introduce the following thermal averages, $\langle S_z\rangle$, $\langle T_z\rangle$, $\langle S_zT_z\rangle$, and $\langle S_z^{t_{2g}}\rangle$ as the mean fields. We assume the type of the orbital ordering as shown in Fig. 1 where the $3d_{3x^2-r^2}$ and $3d_{3y^2-r^2}$ orbitals are alternately ordered, because this type of the ordering is suggested by the cooperative JT distortion observed in $LaMnO_3$.[12]

Figures 2(a) and 2(b) show the magnetic phase diagrams in the parameter space of $(J_{t_{2g}}-t_0)$ and $(J_{t_{2g}}-K)$, respectively. The other energy parameters are used as $U=7$ eV, $U'=5$ eV, and $J=2$ eV throughout the present calculation. As seen in Fig. 2, the A-AF phase appears in a narrow parameter region between the ferromagnetic (F) and G-AF phases. The region of the A-AF phase extends with increasing the values of t_0, $|K|$ and $J^{t_{2g}}$. As we mention in the previous section, the ferromagnetic interaction is induced by the kinetic exchange processes in the presence of the multi-orbitals and the interorbital exchange interaction J. The Hund coupling tends to enhance the magnitude of the ferromagnetic interaction. On the other hand, the antiferromagnetic interaction occurs in the following three terms, $H_{t_{2g}}$, $H_{U'+J}$, and H_U. We confirm that the A-AF phase in Fig. 2 is caused by the competition between these ferromagnetic and antiferromagnetic interactions.

In $LaMnO_3$, t_0 is estimated by the photoemission experiments to be $t_0=V_{pd_\sigma}^2/\Delta\sim 0.72$ eV,[24] where Δ is the energy difference between the occupied O $2p$ and unoccupied Mn $3d$ levels. $|K|$ is expected to be much larger than the crystalline-field splitting (~ 1 eV), since $LaMnO_3$ is in the high spin state. $J^{t_{2g}}$ is estimated to be 0.8 meV from the value of the Néel temperature T_N of the G-AF phase in $CaMnO_3$ (Ref. 10) in the mean-field approximation. When t_0 and K are fixed to these experimental values, the A-AF phase appears in the parameter region where $J^{t_{2g}}$ is slightly larger than the value estimated above. Considering the approximations introduced here, however, we conclude that the theory reproduces this phase well.

Several authors[29–31] have neglected the orbital dependence of the electron transfer and thus did not consider the role of the $(3x^2-r^2/3y^2-r^2)$-type orbital ordering in the spin structure. However, the dependence is of crucial importance to obtain the A-AF state. In order to demonstrate the roles, we calculate the transition temperatures (T_c) of the spin ordered phases and compare them with those obtained by utilizing the simplified model introduced below. In Fig. 3, we present T_c's of the several spin ordered phases obtained by the effective Hamiltonian. The parameter values are chosen as $t_0=0.75$ eV and $K=-3$ eV, and $(3x^2-r^2/3y^2-r^2)$-type orbital ordering is taken. With increasing the values of $J_{t_{2g}}$, the magnetic structure which has the highest T_c is changed from F to A-AF phase, and finally, T_c of G-AF phase becomes highest. In comparison with results in Fig. 2, the above change in the highest T_c corresponds to the change for the magnetic phases in the ground state with increasing $J_{t_{2g}}$. The values of T_c for the A-AF phase is calculated to be about 0.01 eV which is reasonable as compared with the measured value $T_N=141$ K in $LaMnO_3$.[10,12] On the other hand, in Fig. 3 (inset), T_c's are calculated by using the model where the matrix elements of the electron transfer between two degenerate orbitals, a and b, are assumed as $t_{ij}^{aa}=t_{ij}^{bb}=t_0$ and $t_{ij}^{ab}=t_{ij}^{ba}=0$. Furthermore, we assume the so-called antiferromagnetic-type orbital ordering discussed in Ref. 29 and 31, where the electron alternately occupies the two arbitrary types of the orbitals, a and b. In contrast to the results in Fig. 3, T_c of the A-AF phase is always lower than

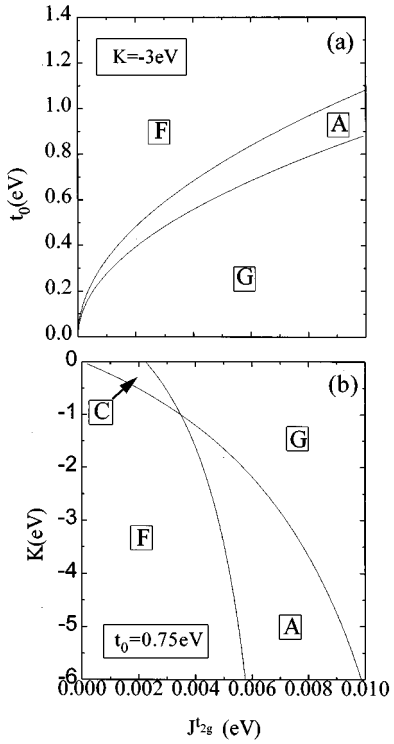

FIG. 2. The magnetic phase diagrams under the $(3x^2-r^2/3y^2-r^2)$-type orbital ordering in the parameter space of (a) $(J_{t_{2g}}-t_0)$ and (b) $(J_{t_{2g}}-K)$, respectively. A, C, and G denotes the A-type, C-type, and G-type antiferromagnetic phase, respectively, and F denotes the ferromagnetic phase.

the other ones. Therefore, A-AF phase is not realized in the simplified model. These results show that the $(3x^2-r^2/3y^2-r^2)$-type ordering and the orbital dependence of the electron transfer are essential to realize the A-AF structure. As we mentioned in the previous section, the electron hopping processes between the nearest-neighbor occupied and unoccupied e_g orbitals cause the ferromagnetic interaction. In the $(3x^2-r^2/3y^2-r^2)$-type ordering, magnitudes of the electron transfer between the occupied $3x^2-r^2(3y^2-r^2)$ orbital and its nearest-neighbor unoccupied $y^2-z^2(z^2-x^2)$ orbital in the ab plane becomes much larger than that in the c direction. As a result of the competition between this anisotropic ferromagnetic interaction and the isotropic antiferromagnetic interaction $J^{t_{2g}}$, the A-AF phase is stabilized. We stress the importance of the off-diagonal matrix elements of electron transfer (t_{ij}^{ab}) for the A-AF structure in the manganites.

In Fig. 3, we also show the transition temperature of the $(3x^2-r^2/3y^2-r^2)$-type orbital ordered phase. It is noted that the values are much higher than that of the spin ordering. Because of this, T_c is independent of the magnitude of $J^{t_{2g}}$. The orbital ordering in the actual compounds may occur at the structural phase transition temperature (875 K) (Ref. 10) from the rhombohedral to O' orthorhombic phases accompanied with the JT distortion. The calculated orbital ordering temperature is of the same order as T_c of the structural phase transition. This fact suggests that the orbital ordering brings about the cooperative JT distortion and the structural phase transition through the orbital-lattice interaction.

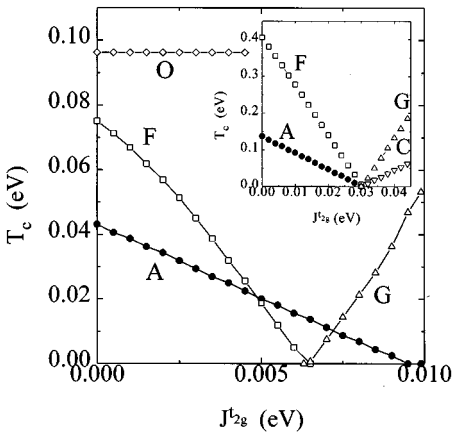

FIG. 3. The transition temperatures of the spin and orbital ordered phases. A, C, G, and F is the transition temperature of the A-type, C-type, and G-type antiferromagnetic and ferromagnetic phases, respectively. O is the transition temperature of the $(3x^2-r^2/3y^2-r^2)$-type orbital ordering. Inset shows the transition temperatures of the magnetic ordered phases in the case of $t_{IJ}^{aa}=t_{ij}^{bb}=t_0$ and $t_{ij}^{ab}=t_{ij}^{ba}=0$. The antiferromagnetic-type orbital ordering is assumed.

In $LaMnO_3$, the JT-type lattice distortion is observed. To study the stability of the A-AF phase under the lattice distortion, we investigate changes in the phase diagram by the modulation of the electron transfer and the level splitting between e_g orbitals due to the lattice distortion. We consider the cooperative JT lattice distortion in the MnO_6 octahedrons. The change in the electron transfer is represented by a parameter R defined by $R=V_{pd\sigma}^S/V_{pd\sigma}^L$, where $V_{pd\sigma}^S$ and $V_{pd\sigma}^L$ are $V_{pd\sigma}$'s for the four short and two long Mn-O bonds in the octahedrons, respectively. Considering that $J^{t_{2g}}$ results from the fourth-order processes with respect to the electron transfer between O $2p$ and Mn $3d$ t_{2g} orbitals, we take a ratio of $J^{t_{2g}}$ in the ab plane to that in the c direction as $J_c^{t_{2g}}/J_{ab}^{t_{2g}}=R^2$. The level splitting due to the JT distortion is also introduced in $H_{\text{2-sites}}$. Because an electron virtually hops from occupied to unoccupied orbitals in the perturbational process for the $H_{U'\pm J}$ term, the energy splitting g is added to the denominators of their energy prefactors. The calculated results are presented in Fig. 4. Parameter values used are the same as those in Fig. 2(a). With increasing R and g, the area of the A-AF phase extends and shifts to the region with larger t_0. This change in the phase diagram with increasing R and g is interpreted as follows. The modification in $V_{pd\sigma}$ enhances the ferromagnetic interaction in the c direction and stabilizes the F phase, on the other hand, the change in $J^{t_{2g}}$ makes the A-AF phase stable. Moreover, introduction of g weakens the ferromagnetic interaction, due to suppression of the interorbital exchange processes. As a result of competition between above three contributions, the stability of A-AF phase is strengthened with increasing R and g. We conclude that the A-AF phase is still stable under the JT lattice distortion.

In the next, we examine the excitations in the spin and orbital degrees of freedom in the A-AF state accompanied with the $(3x^2-r^2/3y^2-r^2)$-type orbital ordering. In order to calculate the excitations, we adopt an extended cell which consists of four Mn ions as a unit cell. The large Hund cou-

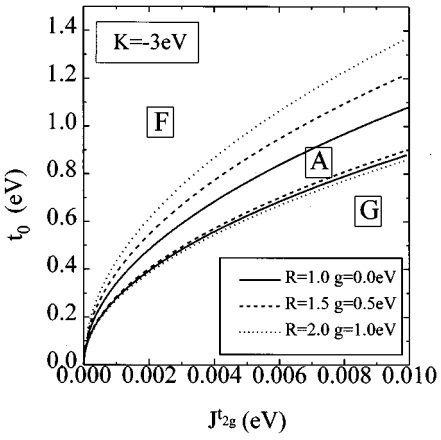

FIG. 4. The magnetic phase diagram under the $(3x^2-r^2/3y^2-r^2)$-type orbital ordering with effects of the lattice distortion. A and G denote the A-type and G-type antiferromagnetic phases, respectively, and F denotes the ferromagnetic phase. R represents the modifications of t_0 and $J^{t_{2g}}$, and g denotes the energy splitting. The solid, dashed, and dotted lines show the phase boundary for the three sets of the parameter values.

pling makes e_g and t_{2g} spins precess in phase in the low-energy states. Therefore, we introduce a spin operator $\mathbf{J}_i$ with $J=2$, replace the spin operators $\mathbf{S}_i$ and $\mathbf{S}_i^{t_{2g}}$ with $\mathbf{S}_i=(1/4)\mathbf{J}_i$ and $\mathbf{S}_i^{t_{2g}}=(3/4)\mathbf{J}_i$, and eliminate H_K. The conventional Holstein-Primakoff transformation is applied to the spin and pseudospin operators in the Hamiltonian, and the two kinds of the boson operators, σ_i and τ_i are introduced for the spin and orbital excitations, respectively. We rewrite the Hamiltonian by using the boson operators and retain up to second-order terms of σ_i and τ_i and their cross terms. The cross terms of σ_i and τ_i express the interaction between the excitations in the spin and orbital degrees of freedom. We adopt the mean-field approximation in these terms and their values are determined self-consistently.

In Fig. 5, theoretical and experimental results of the dispersion relation of the spin waves are presented. Parameters are chosen as $K=-3$ eV, and $J^{t_{2g}}=0.0065$ eV. The dispersion curves along $A\rightarrow B$ correspond to those in $(0,0,0)\rightarrow(\pi/a,\pi/a,0)$ direction, and the curves along $A\rightarrow C$ correspond to those in $(0,0,0)\rightarrow(0,0,\pi/a)$ direction in the Brillouin zone for the cubic structure with a being the lattice constant. With increasing t_0, the slope in the $A\rightarrow B$ direction increases, on the other hand, that in the $A\rightarrow C$ direction decreases. To see the dependence on t_0, we consider the following layer-type Heisenberg model with $S=2$, i.e., $H=(J_{ab}\Sigma_{\langle ij\rangle}^{ab}+J_c\Sigma_{\langle ij\rangle}^{c})\mathbf{S}_i\cdot\mathbf{S}_j$, $(J_{ab}<0,\ J_c>0)$, the spin-wave dispersion relation in the A-AF phase of this model is given near the $(0,0,0)$ point by $\epsilon(\mathbf{k})=4\sqrt{-J_{ab}J_c a^2(k_x^2+k_y^2)+J_c^2a^2k_z^2}$. With increasing t_0, $|J_{ab}|$ increases and $|J_c|$ decreases, as we pointed out previously. Therefore, we obtain that the slopes in the ab plane and the c directions increases and decreases, respectively. Experimental results in $LaMnO_3$ obtained by the neutron-scattering experiment are indicated by the open circles.[33] The bandwidths of the spin wave are experimentally estimated to be about 32 and 5 meV in the ab plane and the c direction, respectively, suggesting the two-dimensional character in the spin system. Apart from the energy gap in the spin waves which is neglected in the present calculation, we find good agreement between theory and experiment. The anisotropic character in the spin system originates from the strong ferromagnetic interaction in the ab plane due to $H_{U'-J}$ and the weak antiferomagnetic one in the c direction due to $J^{t_{2g}}$. The electron correlation and the orbital degrees of freedom play the crucial roles on the excitations in the spin system, as well as the ground states.

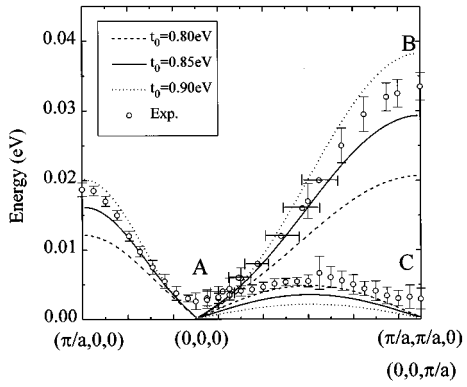

FIG. 5. The dispersion relations of the spin wave. The open circles show the results obtained by the neutron-scattering experiment (Ref. 33). Note that lines along $(0,0,0)\rightarrow(\pi/a,\pi/a,0)$ and $(0,0,0)\rightarrow(0,0,\pi/a)$ are shown on the same axis.

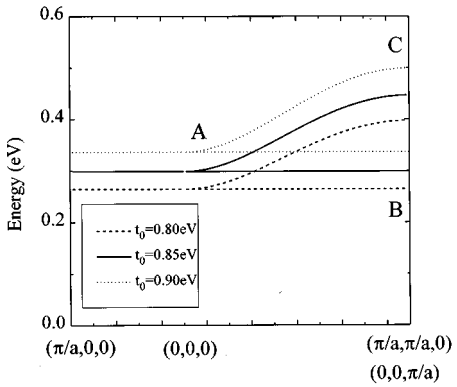

FIG. 6. The dispersion relations of the orbital wave. Note that lines along $(0,0,0)\rightarrow(\pi/a,\pi/a,0)$ and $(0,0,0)\rightarrow(0,0,\pi/a)$ are shown on the same axis.

The orbital excitations from the $(3x^2-r^2/3y^2-r^2)$-type orbital ordering described by τ_i are called the orbital wave, which interacts with the spin wave and their dispersion relations have influence on each other. In Fig. 6, we show the calculated results of the dispersion relation of the orbital wave for several values of t_0. The other parameter values are the same as those in Fig. 5 and the spin structure in the ground state is taken to be the A-AF state. With increasing t_0, the bandwidth of the orbital wave monotonically increases, in contrast to the case of the spin wave. An energy gap in the orbital wave appears and also increases with t_0. Magnitude of the energy gap is the same order of the bandwidth: $t_0^2/(U'-J)$. The energy gap in the orbital wave is caused by the layer type spin structure (A-AF) in the ground state through the interaction between the spin and the orbital in the effective Hamiltonian. In the A-AF phase, the nearest-

neighbor spin correlation in the ab plane is different from that along the c direction. As a result, an anisotropic interaction between the nearest-neighboring pseudospins is brought about. It is noted that the nature of the energy gap in the orbital wave strongly depends on the spin structure. The characteristic feature in the orbital wave appears in the flatness of the dispersion in the ab plane. The dispersion in the orbital wave is controlled by the terms $t_{ij}^{aa}t_{ij}^{bb}(T_{i+}T_{j-}+T_{i-}T_{j+})$ and $t_{ij}^{ab}t_{ij}^{ba}(T_{i+}T_{j+}+T_{i-}T_{j-})$ in the effective Hamiltonian, where the both coefficients, $t_{ij}^{aa}t_{ij}^{bb}$ and $t_{ij}^{ab}t_{ij}^{ba}$, become zero in the ab plane for the $(3x^2-r^2/3y^2-r^2)$ orbital ordering. Thus, the flat dispersion in the ab plane is characteristic of the $(3x^2-r^2/3y^2-r^2)$-type orbital ordering. It is possible to directly observe the orbital wave by using the light-scattering and the electron-scattering techniques in analogy with the two-magnon Raman scattering in magnetic compounds. Through the observation and analysis of the characteristic nature of the orbital waves, important information about the orbital ordered phase and its relation to the magnetic ordering may be obtained.

IV. SUMMARY

In this paper, we have derived the effective Hamiltonian to investigate the electronic structure in the manganites of perovskite structure. In this Hamiltonian, the doubly degenerate e_g orbitals and the electron-electron interactions in these orbitals are taken into account. Also, Hund coupling interaction and the antiferromagnetic interaction between the nearest-neighbor t_{2g} spins are introduced. The Hamiltonian is represented by the conventional spin operator for spin, the pseudospin operator for orbital, and the restricted electron operator due to the electron-electron interactions. The product of the spin and orbital parts in this model implies the strong coupling between the orbital and spin structures. The competition and interplay between the spin and orbital degrees of freedom brings about rich phenomena in this system.

The results of the calculations in the undoped system and their implications are summarized as follows. We calculated the phase diagrams and the transition temperatures for the spin and orbital ordered states in the mean-field approximation. The A-type antiferromagnetic structure comes out by the competition between the antiferromagnetic interaction between t_{2g} spins and the anisotropic ferromagnetic interaction induced by the virtual electron hopping in the e_g orbitals. We stress the importance of the $(3x^2-r^2/3y^2-r^2)$-type orbital ordering and the orbital dependence of the electron transfer for stabilization of the A-AF ground state. The excitations in the spin and orbital degrees of freedom were calculated in the spin-wave approximation. The calculated dispersion relation of the spin waves well reproduces the experimental results. The anisotropic nature of the spin excitations reflects the strong ferromagnetic interaction in the ab plane and the weak antiferromagnetic one in the c direction due to the orbital ordering. The characteristic features in the dispersion relation and the energy gap of the orbital waves, which originate from the $(3x^2-r^2/3y^2-r^2)$-type orbital ordering and the A-AF spin ordering, were pointed out.

The effective Hamiltonian in Eq. (2.4) may also be applied to the doped system where $H_{U'-J}$ is the leading term in $\tilde{H}_{e_g}$ as seen in the undoped systems. The study in the doped system will be presented in a separate publication.

ACKNOWLEDGMENTS

S.I. is financially supported by the Japan Society for the Promotion of Science. This work was supported by Priority-Area Grants from the Ministry of Education, Science and Culture of Japan, and the New Energy and Industrial Technology Development Organization (NEDO). Parts of the numerical calculations have been performed at the Supercomputing Center of Institute for Materials Research, Tohoku University. We would like to thank to Professor A. J. Millis, Professor Y. Endoh, Dr. K. Hirota, Dr. T. Mizokawa, Dr. W. Koshibae, Mr. S. Okamoto, and Y. Kawamura for their valuable discussions.

*Current address: Department of Applied Physics, University of Tokyo, Tokyo, 113, Japan.

[1] K. Chahara, T. Ohono, M. Kasai, Y. Kanke, and Y. Kozono, Appl. Phys. Lett. **62**, 780 (1993); K. Chahara, T. Ohono, M. Kasai, and Y. Kozono, *ibid*. **63**, 1990 (1993).

[2] R. von Helmolt, J. Wecker, B. Holzapfel, L. Schultz, and K. Samwer, Phys. Rev. Lett. **71**, 2331 (1993).

[3] Y. Tokura, A. Urushibara, Y. Moritomo, T. Arima, A. Asamitsu, G. Kido, and N. Furukawa, J. Phys. Soc. Jpn. **63**, 3931 (1994); A. Urushibara, Y. Moritomo, T. Arima, A. Asamitsu, G. Kido, and Y. Tokura, Phys. Rev. B **51**, 14 103 (1995).

[4] S. Jin, T. H. Tiefel, M. McCormack, R. A. Fastnacht, R. Ramesh, and L. H. Chen, Science **264**, 413 (1994).

[5] R. M. Kusters, J. Singleton, D. A. Keen, R. McGreevy, and W. Hayes, Physica B **155**, 362 (1989).

[6] G. H. Jonker and H. van Santen, Physica **16**, 337 (1950); G. H. Jonker, *ibid*. **22**, 707 (1956).

[7] A. Asamitsu, Y. Moritomo, Y. Tomioka, T. Arima, and Y. Tokura, Nature (London) **373**, 407 (1995).

[8] Y. Tomioka, A. Asamitsu, Y. Moritomo, H. Kuwahara, and Y. Tokura, Phys. Rev. Lett. **74**, 5108 (1995).

[9] E. O. Wollan and W. C. Koehler, Phys. Rev. **100**, 545 (1955).

[10] J. B. Goodenough, Phys. Rev. **100**, 564 (1955); in *Progress in Solid State Chemistry*, edited by H. Reiss (Pergamon, London, 1971), Vol. 5.

[11] J. B. A. A. Elemans, B. van Laar, K. R. van der Veen, and B. O. Loopstra, J. Solid State Chem. **3**, 238 (1971).

[12] G. Matsumoto, J. Phys. Soc. Jpn. **29**, 606 (1970).

[13] C. Zener, Phys. Rev. **82**, 403 (1951).

[14] P. W. Anderson and H. Hasegawa, Phys. Rev. **100**, 675 (1955).

[15] P. G. de Gennes, Phys. Rev. **118**, 141 (1960).

[16] K. Kubo and N. Ohata, J. Phys. Soc. Jpn. **33**, 21 (1972); K. Kubo, *ibid*. **33**, 929 (1972).

[17] N. Furukawa, J. Phys. Soc. Jpn. **64**, 2734 (1996); **64**, 3164 (1996).

[18] A. J. Millis, P. B. Littlewood, and B. I. Shrainman, Phys. Rev. Lett. **74**, 5144 (1995); A. J. Millis, B. I. Shrainman, and R. Mueller, *ibid*. **77**, 175 (1996).

[19] A. J. Millis, Phys. Rev. B **53**, 8437 (199?).

[20] H. Röder, J. Zang, and A. R. Bishop, Phys. Rev. Lett. **76**, 1356

(1996); J. Zang, A. R. Bishop, and H. Röder, Phys. Rev. B **53**, R8840 (1996).

[21] N. Hamada, H. Sawada, and K. Terakura, in *Spectroscopy of Mott Insulators and Correlated Metals*, edited by A. Fujimori and Y. Tokura, Springer Series in Solid State Science Vol. 119 (Springer-Verlag, Berlin, 1995), p. 95.

[22] T. Mizokawa and A. Fujimori, Phys. Rev. B **51**, 12 880 (1995).

[23] J. Inoue and S. Maekawa, Phys. Rev. Lett. **74**, 3407 (1995).

[24] S. Saitoh, A. E. Bocquet, T. Mizokawa, H. Namatame, A. Fujimori, M. Abbate, Y. Takeda, and M. Takano, Phys. Rev. B **51**, 13 942 (1995).

[25] J. Kanamori, J. Phys. Chem. Solids **10**, 87 (1959).

[26] K. I. Kugel and D. I. Khomskii, Pisma Zh. Eksp. Teor. Fiz. **15**, 629 (1972) [JETP Lett. **15**, 446 (1972)]; D. I. Khomskii and K. I. Kugel, Solid State Commun. **13**, 763 (1973); Zh. Eksp. Teor. Fiz. **64**, 1429 (1973) [Sov. Phys. JETP **37**, 725 (1973)]; K. I. Kugel and D. I. Khomskii, Sov. Phys. Usp. **25**, 231 (1982).

[27] S. Ishihara, J. Inoue, and S. Maekawa, Physica C **263**, 130 (1996).

[28] J. C. Slater and G. F. Koster, Phys. Rev. **94**, 1498 (1954); W. A. Harrison, *Electronic Structure and the Properties of Solids, The Physics of the Chemical Bond* (Freeman, San Francisco, 1980).

[29] L. M. Roth, Phys. Rev. **149**, 306 (1966).

[30] M. Cyrot and C. Lyon-Caen, J. Phys. (Paris) **36**, 253 (1975).

[31] S. Inagaki, J. Phys. Soc. Jpn. **39**, 596 (1975).

[32] C. Castellani, C. R. Natoli, and J. Ranninger, Phys. Rev. B **18**, 4945 (1978); T. M. Rice, in *Spectroscopy of Mott Insulators and Correlated Metals*, edited by A. Fujimori and Y. Tokura, Springer Series in Solid-State Science Vol. 119 (Springer-Verlag, Berlin, 1995), p. 221.

[33] K. Hirota, N. Kaneko, A. Nishizawa, and Y. Endoh, J. Phys. Soc. Jpn. **65**, 3736 (1996).